Supporting Information

High Magnetic Coercivity in Nanostructured Mn_3O_4 Thin Films Obtained by Chemical Vapor Deposition

Lorenzo Bigiani,[‡] Mariam Hassan,[†,∥] Davide Peddis,[†] Chiara Maccato,[‡,]*

Gaspare Varvaro,[†,], Cinzia Sada,[§] Elza Bontempi,[#]*

Sara Martí-Sánchez,[⊥] Jordi Arbiol,[⊥,¶] and Davide Barreca[▽]

[‡] *Department of Chemical Sciences, Padova University and INSTM, 35131 Padova, Italy*

[†] *CNR-ISM, Monterotondo Scalo, 00015 Roma, Italy*

[∥] *Department of Matter Sciences and Engineering, Environment and Urban Planning, Marche Polytechnic University, 60121 Ancona, Italy*

[§] *Department of Physics and Astronomy, Padova University and INSTM, Padova, Italy*

[#] *Chemistry for Technologies Laboratory, Department of Mechanical and Industrial Engineering, Brescia University and INSTM, Brescia, Italy*

[⊥] *Catalan Institute of Nanoscience and Nanotechnology (ICN2), CSIC and BIST, Bellaterra, 08193 Barcelona, Catalonia, Spain*

[¶] *ICREA, Pg. Lluís Companys 23, 08010 Barcelona, Catalonia, Spain*

[▽] *CNR-ICMATE and INSTM, Department of Chemical Sciences, Padova University, 35131Padova, Italy*

* Corresponding authors; Phone: +39-0498275234, E-mail: chiara.maccato@unipd.it (C.M.); Phone: +39-0690672651, E-mail: gaspare.varvaro@ism.cnr.it (G.V.).

S-1. X-ray diffraction (XRD)

The texture coefficient (TC_{hkl}) was calculated as:[1-2]

$$TC_{hkl} = (I_{hkl}/I^0_{hkl}) / \{(1/N)*[\Sigma(I_{hkl}/I^0_{hkl})]\} \quad \text{(S1)}$$

where I_{hkl} and I^0_{hkl} are the (hkl) diffracted intensities for the target sample and the reference *haussmannite* Mn_3O_4 pattern, and N is the overall reflection number.[3]

The average crystallite sizes (D) were estimated from the patterns presented in Figure S1 by using the Scherrer formula:[1,4-14]

$$D = 0.9[\lambda/(FWHM*\cos\theta)] \quad \text{(S2)}$$

where $\lambda = 0.15418$ nm is the used excitation wavelength, whereas FWHM and 2θ are the full width at half maximum and position, respectively, for the observed diffraction peaks.

The dislocation density (δ) values were evaluated through the following equation:[1,4,7,15-16]

$$\delta = 1/D^2 \quad \text{(S3)}$$

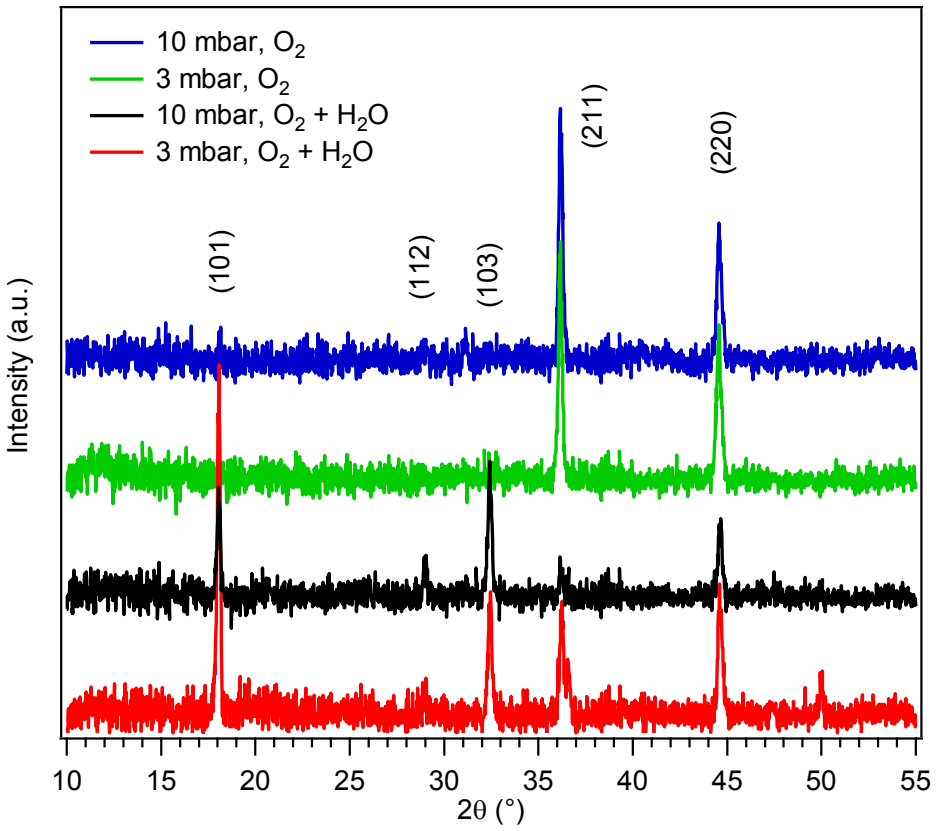

Figure S1. XRD patterns of Mn_3O_4 thin films deposited under different experimental conditions. Miller indexes are referred to the diffraction peaks of tetragonal α-Mn_3O_4 (*hausmannite*).[3]

S-2. Field emission-scanning electron microscopy (FE-SEM)

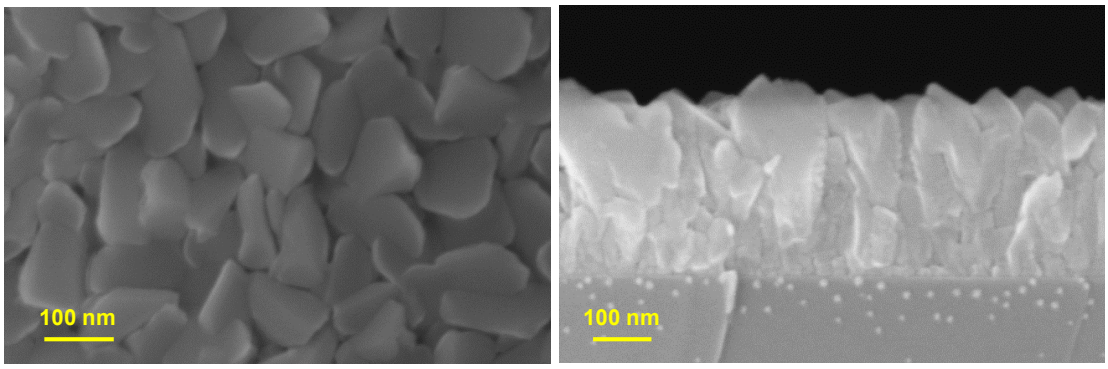

Figure S2. Plane-view (left) and cross-sectional (right) FE-SEM micrographs for a Mn_3O_4 film deposited at 10.0 mbar in O_2+H_2O.

S-3. Transmission electron microscopy (TEM) and electron energy loss spectroscopy (EELS)

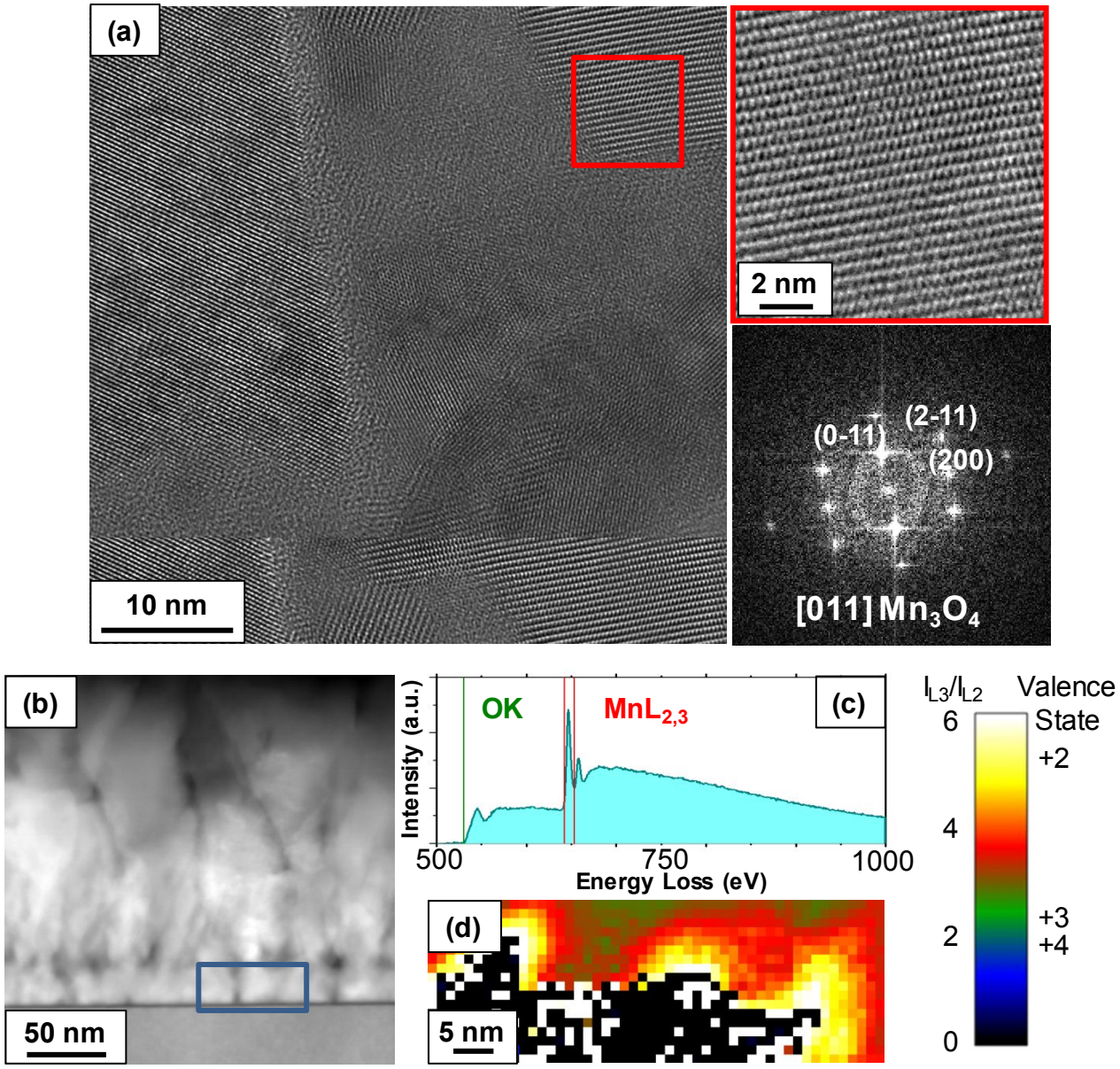

Figure S3. TEM analyses performed on a Mn_3O_4 specimen deposited on Si(100) at 10 mbar in O_2+H_2O. (a) HR-TEM micrographs showing the Mn_3O_4/Si(100) interface. A higher resolution image and the indexed power spectrum for the red squared area are also displayed. (b) Low magnification cross-sectional HAADF-STEM image. (c) O and Mn EELS signals on the region marked in (b). (d) Corresponding oxidation state map. The black color corresponds to a saturated region, too thick to obtain any clear signal.

S-4. Secondary ion mass spectrometry (SIMS)

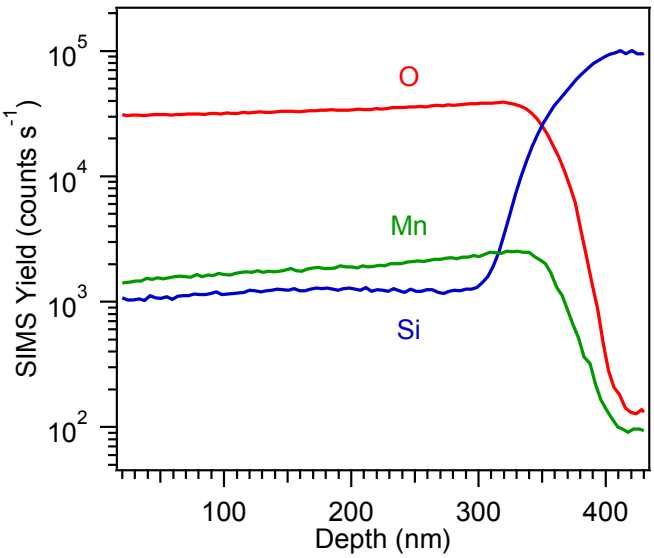

Figure S4. Representative SIMS depth profile for a Mn_3O_4 thin film deposited at 10.0 mbar in dry O_2.

S-5. Magnetic measurements

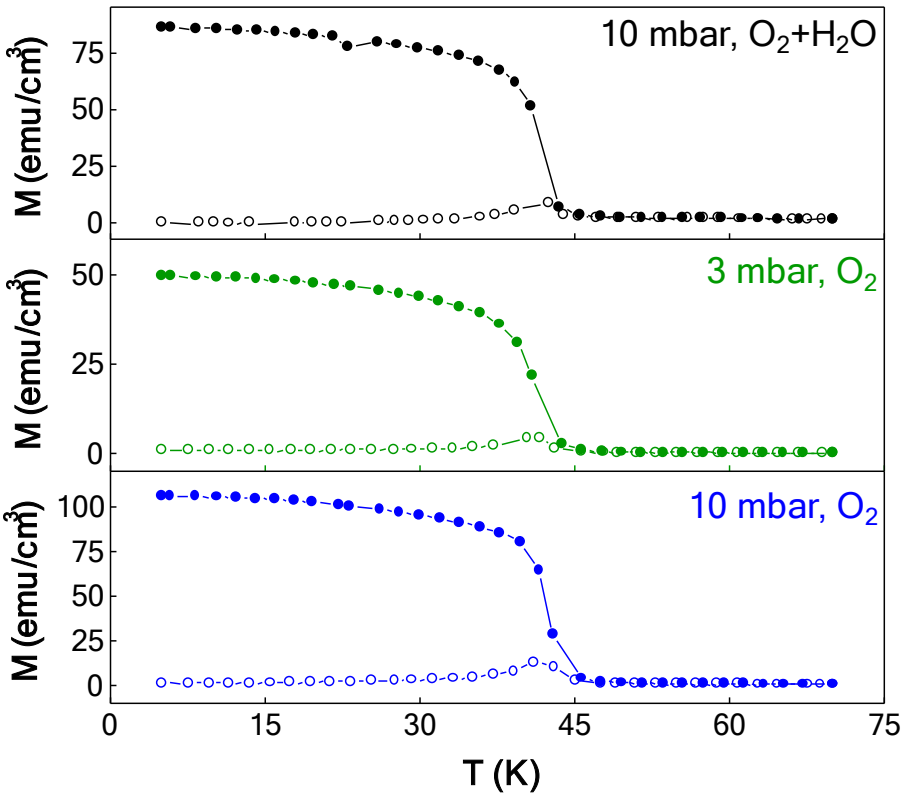

Figure S5. FC (–●–) and ZFC (–○–) curves of various Mn_3O_4 specimens measured under a magnetic field of 20 mT applied in the film plane.

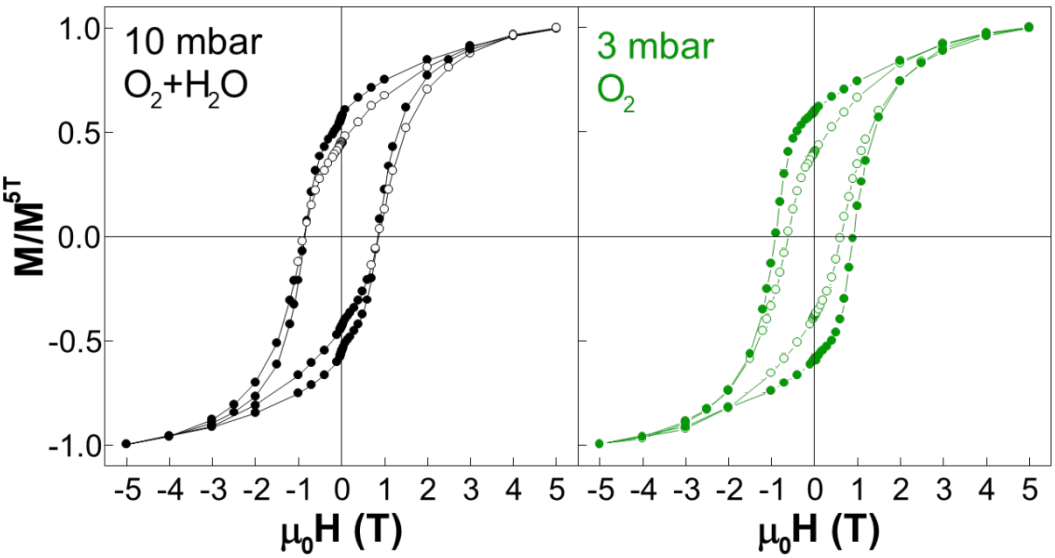

Figure S6. Low temperature (5 K) in-plane (–●–) and out-of-plane (–○–) field-dependent magnetization loops of two different Mn_3O_4 samples. The magnetization axis is normalized to the magnetization value at H = 5T (M^{5T}).

■ REFERENCES

(1) Larbi, T.; Ouni, B.; Boukhachem, A.; Boubaker, K.; Amlouk, M. Investigation of Structural, Optical, Electrical and Dielectric Properties of Catalytic Sprayed Hausmannite Thin Film. *Mater. Res. Bull.* **2014**, *60*, 457-466.

(2) Bigiani, L.; Barreca, D.; Gasparotto, A.; Sada, C.; Martí-Sanchez, S.; Arbiol, J.; Maccato, C. Controllable Vapor Phase Fabrication of F:Mn_3O_4 Thin Films Functionalized with Ag and TiO_2. *CrystEngComm* **2018**, *20*, 3016-3024.

(3) Pattern N° 024-0734, JCPDS (2000).

(4) Amara, M. A.; Larbi, T.; Labidi, A.; Karyaoui, M.; Ouni, B.; Amlouk, M. Microstructural, Optical and Ethanol Sensing Properties of Sprayed Li-Doped Mn_3O_4 Thin Films. *Mater. Res. Bull.* **2016**, *75*, 217-223.

(5) Dubal, D. P.; Dhawale, D. S.; Salunkhe, R. R.; Fulari, V. J.; Lokhande, C. D. Chemical Synthesis and Characterization of Mn_3O_4 Thin Films for Supercapacitor Application. *J. Alloys Compd.* **2010**, *497*, 166-170.

(6) Dubal, D. P.; Dhawale, D. S.; Salunkhe, R. R.; Pawar, S. M.; Lokhande, C. D. A novel Chemical Synthesis and Characterization of Mn_3O_4 Thin films for Supercapacitor Application. *Appl. Surf. Sci.* **2010**, *256*, 4411-4416.

(7) Larbi, T.; Lakhdar, M. H.; Amara, A.; Ouni, B.; Boukhachem, A.; Mater, A.; Amlouk, M. Nickel Content Effect on the Microstructural, Optical and Electrical Properties of p-type Mn_3O_4 Sprayed Thin Films. *J. Alloys Compd.* **2015**, *626*, 93-101.

(8) Belkhedkar, M. R.; Ubale, A. U. Physical Properties of Nanostructured Mn_3O_4 Thin Films Synthesized by SILAR Method at Room Temperature for Antibacterial Application. *J. Mol.*

Struct. **2014**, *1068*, 94-100.

(9) Scialabba, C.; Puleio, R.; Peddis, D.; Varvaro, G.; Calandra, P.; Cassata, G.; Cicero, L.; Licciardi, M.; Giammona, G. Folate Targeted Coated SPIONs as Efficient Tool for MRI. *Nano Res.* **2017**, *10*, 3212-3227.

(10) Yadav, A. A.; Jadhav, S. N.; Chougule, D. M.; Patil, P. D.; Chavan, U. J.; Kolekar, Y. D. Spray Deposited Hausmannite Mn_3O_4 Thin Films Using Aqueous/Organic Solvent Mixture for Supercapacitor Applications. *Electrochim. Acta* **2016**, *206*, 134-142.

(11) Najim, A. A.; Darwoysh, H. H.; Dawood, Y. Z.; Hazaa, S. Q.; Salih, A. T. Structural, Topography, and Optical Properties of Ba-Doped Mn_3O_4 Thin Films for Ammonia Gas Sensing Application. *Phys. Status Solidi A* **2018**, *215*, 1800379.

(12) Larbi, T.; Ben Said, L.; Ben Daly, A.; Ouni, B.; Labidi, A.; Amlouk, M. Ethanol Sensing Properties and Photocatalytic Degradation of Methylene Blue by Mn_3O_4, $NiMn_2O_4$ and Alloys of Ni-Manganates Thin Films. *J. Alloys Compd.* **2016**, *686*, 168-175.

(13) Kocyigit, A. Structural, Optical and Electrical Characterization of Mn_3O_4 Thin Films via Au Composite. *Mater. Res. Express* **2018**, *5*,

(14) Xia, Y.; Qiang, Z.; Lee, B.; Becker, M. L.; Vogt, B. D. Solid State Microwave Synthesis of Highly Crystalline Ordered Mesoporous Hausmannite Mn_3O_4 Films. *CrystEngComm* **2017**, *19*, 4294-4303.

(15) Shaikh, A. A.; Waikar, M. R.; Sonkawade, R. G. Effect of Different Precursors on Electrochemical Properties of Manganese Oxide Thin Films Prepared by SILAR Method. *Synth. Met.* **2019**, *247*, 1-9.

(16) Bayram, O.; Guney, H.; Ertargin, M. E.; Igman, E.; Simsek, O. Effect of Doping Concentration on the Structural and Optical Properties of Nanostructured Cu-Doped Mn_3O_4 Films Obtained by SILAR Technique. *Appl. Phys. A* **2018**, *124*, 606.